Jurnal Teknologi

Full Paper

FULL SCALE STATIC LOAD TEST ON THE SPIDER NET SYSTEM

Helmy Darjanto[a*], Masyhur Irsyam[b], Sri Prabandiyani Retno[a]

[a]Civil Engineering Department, Diponegoro University, Semarang, Indonesia
[b]Civil Engineering Department, Institute of Technology Bandung, Bandung, Indonesia

Article history
Received
3 August 2015
Received in revised form
31 August 2015
Accepted
23 September 2015

*Corresponding author
hdarjanto@gmail.com

Graphical abstract

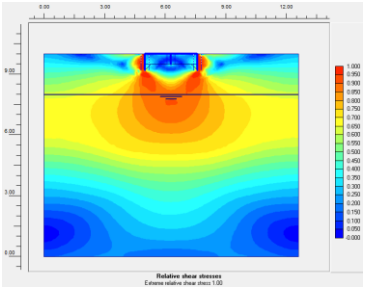

Abstract

The Spider Net System Footing (SNSF) is a raft foundation system that commonly used in Indonesia. It contains a plate, downward ribs system for reinforcement, and the compacted filled soil. The ribs are in longitudinal and transversal, called as settlement rib and in diagonal direction, named as construction rib. This paper explores the load transfer mechanism along the plate, the ribs, filled soil and the base soil under the footing system. The mechanism is investigated by conducting full scale static load test on SNSF. Strain gauges were installed to monitor the strain increment of each footing elements during loading. 3D numerical analysis was also conducted to verify the experimental results. To analyze the results, Load-Ultimate Ratio Factor (L-URF) was proposed. L-URF was a ratio between ultimate soil bearing capacity of the SNSF and the applied loading at specific element. Higher the L-URF value means higher loading applied at its associate element. Both experimental and numerical results show that at the first stage the loading was fully carried out by the tip of the ribs and transferred to the soil stratum under the footing system. Increasing the loading, the ribs, plate, and filled soil altogether sustain the loading and then transferred to the soil stratum below the footing system. The results also affirm that SNSF generate higher bearing capacity compare with simple shallow footing.

Keywords: SNSF, load transfer mechanism, load-ultimate ratio factor, rib

Abstrak

Sistem Tapak Sarang Labah-Labah (SNSF) adalah asas rakit yang biasanya digunakan di Indonesia. Ia mengandungi satu plat, sistem rusuk bawah untuk tetulang, dan tanah yang dipenuhi dengan tanah yang dipadatkan. Rusuk itu berada dalam keadaan membujur dan melintang dipanggil sebagai rusuk enapan dan dalam arah pepenjuru dinamakan sebagai rusuk pembinaan. Kertas kerja ini meneroka mekanisme pemindahan beban sepanjang plat, rusuk, tanah yang memenuhi dan tanah asas di bawah sistem tapak. Mekanisme ini disiasat dengan menjalankan ujian beban statik skala penuh pada SNSF. Tolok terikan telah dipasang untuk memantau kenaikan tekanan setiap unsur-unsur asas semasa pembebanan. Analisis berangka 3D juga telah dijalankan untuk mengesahkan keputusan ujikaji. Untuk menganalisis keputusan, Nisbah beban-Faktor Muktamad (L-urf) telah dicadangkan. L-urf adalah nisbah antara keupayaan galas tanah utama SNSF dan beban kenaan pada unsur tertentu. Nilai L-urf yang lebih tinggi bermakna muatan yang lebih tinggi dikenakan pada unsur sekutunya. Kedua-dua keputusan ujikaji dan berangka menunjukkan bahawa peringkat pembenanan pertama telah diambil sepenuhnya oleh hujung rusuk dan dipindahkan ke lapisan tanah di bawah sistem tapak. Dengan berterusan pembebanan, rusuk, plat, dan tanah yang memenuhi bersama-sama menahan beban dan kemudian dipindahkan ke lapisan tanah di bawah sistem tapak. Keputusan juga menunjukkan bahawa SNSF menjana keupayaan galas yang lebih tinggi berbanding dengan tapak cetek biasa.

Kata kunci: SNSF, mekanisme beban pemindahan, nisbah beban faktor muktamad, rusuk

1.0 INTRODUCTION

Spider net System Footing (SNSF) is an innovated raft footing originally from Indonesia. It comprises of a raft plate and ribs system to improve the footing stiffness. The footing is commonly constructed for less than 6 stories building. The ribs are in longitudinal and transversal that called settlement rib and in diagonal direction named construction rib. They divide the plate into smaller square segments. The space confined by the ribs system and the plate is filled with compacted soil. Detail illustration of SNSF can be revealed in Figure 1.

Suhendro [1] investigated raft foundation supported by short piles and developed a numerical soil-structure interaction model among slab, pipe and soils utilizing Non-linear 3D Finite Element Method. Hardiyanto *et al*. [2] proposed a combination of beam on elastic foundation equations and resistant moments on the claws elements of claw footing system to calculate its bearing capacity.

Regarding to the footing settlements, Anderson *et al*. [3] conducted full scale static load test on the shallow footing lying on the sand. Their results agreed with traditional elastic settlement theory. Srilakshmi and Rekha [4] simulated 2D axisymmetric finite element model to investigate failure pattern of mat foundation. Djajaputra *et al*. [5] also run a full scale static load test on the shallow footing at the apron and taxiway of Tarakan Airport. They confirm that the results were in accordance to Terzaghi and Winkler theory for elastic deformation. Among all, [5] was the one who work on SNSF, however they left the load transfer mechanism beyond the scope. This works intend to report the results of full scale static load test (SLT) on a segment of SNSF, especially related to element stress strain behavior during loading.

(a) Segments with construction and settlement ribs

(b) The compaction of filled soil

(c) The raft plate construction

Figure 1 SNSF construction [6]

2.0 FIELD CONDITION

The location of the full scale SLT was next to Demak – Semarang highway. The location support heavy equipment mobility for the test. Both field and laboratory tests were conducted to investigate the soil layer condition.

2.1 Field Tests

Cone Penetration Test (CPT – Sondir test) and Standard Penetration Test (SPT) were conducted until 15 m depth. The results are presented in Figure 2 and Figure 3. It shows that the soil is soft soil with corrected SPT (NSPT) value less than 6. The bore log shows that the soils were almost uniform silty clay excepting the 0.5 m first depth.

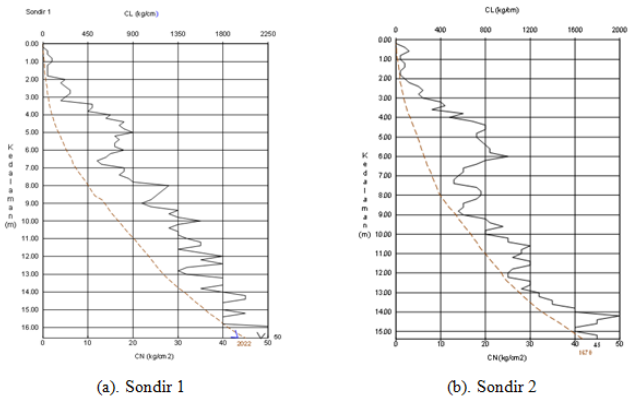

Figure 2 CPT results

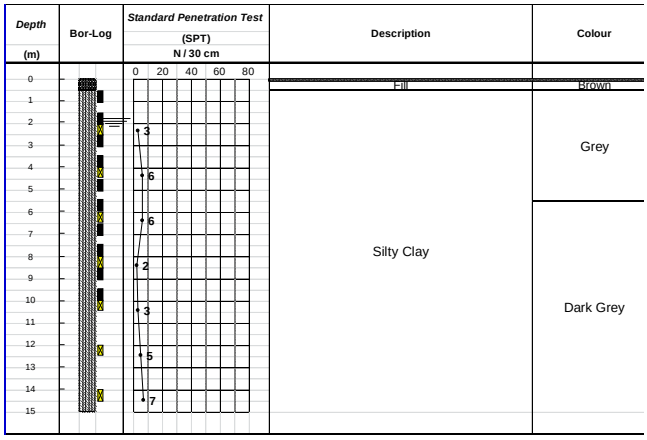

Figure 3 Bore log B1

2.2 Laboratory Tests

The grain size distribution of the soil can be seen in Figure 4. It clearly shows that the soils were silty clay as well as bore log results. Meanwhile, the physical and index properties are presented in Table 1 and Table 2. The plasticity indexes of the soil were higher than 35%. High plasticity index is associated with the swelling potential of the soil with the water variation [7].

The oedometer test was conducted to explore the primary consolidation behavior. The compression coefficient of the soil is relatively high as well as the recompression one, especially for soil layer at 3.5 m depth that has Over Consolidated Ratio (OCR) of 9 (Table 3).

To investigate the shear strength parameter, the Consolidated Undrained (CU) triaxial test was conducted. Two samples from 3 m and 5 m depth were tested. The cohesion c and the internal friction angle φ are 25.78 kpa and 10.74° for 3 m depth and 27.10 kpa and 13.84° for 5 m depth.

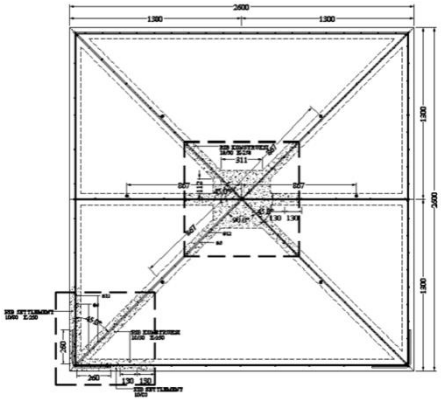

Figure 4 2.6 m × 2.6 m SNSF sample

Table 1 Physical properties of the soils

No.	Depth (m)	γ_{sub} (ton/m³)	γ_{dry} (ton/m³)	w (%)	G_s	e	n (%)	S_r (%)
1	1.5 - 2	1.697	1.138	49.03	2.652	1.300	56.50	-
		1.586	1.199	32.23	2.514	1.096	52.29	73.93
2	3 – 3.5	1.705	1.162	46.65	2.585	1.324	57.00	-
		1.665	1.586	40.46	2.620	1.210	54.76	87.59
3	3.5 - 4	1.781	1.354	31.50	2.524	1.076	46.34	92.05
4	5 - 6	1.749	1.259	38.98	2.634	0.858	52.21	93.97

Table 2 Index properties and soil classification

No.	Depth (m)	LL (%)	PL (%)	PI (%)	Note
1	1.5 - 2	86.45	26.07	60.38	Plasticity Chart (1998): Inorganic clays of high plasticity
2	3 - 3.5	92.50	25.51	66.99	Plasticity Chart (1998): Inorganic clays of high plasticity
3	3.5 - 4	82.44	23.06	59.38	Plasticity Chart (1998): Inorganic clays of high plasticity
4	5 - 5.5	90.00	29.39	60.60	Plasticity Chart (1998): Inorganic clays of high plasticity
5	5.5 - 6	114.13	29.43	84.70	Plasticity Chart (1998): Inorganic clays of high plasticity

Table 3 Consolidation parameters

No.	Depth (m)	γ_{sat} (ton/m³)	γ' (ton/m³)	e	p_0 (kg/cm²)	p_p (kg/cm²)	c_c	c_s
1	3.5 - 4	1.787	0.79	1.076	0.31	2.52	0.429	0.149
2	5.5 - 6	1.820	0.82	0.858	0.49	1.48	0.350	0.077

3.0 EXPERIMENTAL SETUP

3.1 Sample Preparation

The SNSF sample detail is shown in Figure 5. The SNSF construction required to excavate 3m × 3m ground with 0.5m depth. It was followed by making the form work at the excavated area. The floor of the ribs form work was about 30 cm width to 5 cm thickness of 1:5 mixed cement-sand. The reinforcements were installed when the ribs scaffolding was ready. Two types of strain gauges were installed. They were FLA-5-11 and PL-60-11 that were installed at reinforced steel bars and concrete surface respectively. They were installed both at the ribs and the plate. Detail strain gauges installation can be revealed in Figure 6 and Figure 7. Once the instrument installation completed, concrete casting started with construction ribs following by settlement ribs using fc'= 21 MPa concrete types.

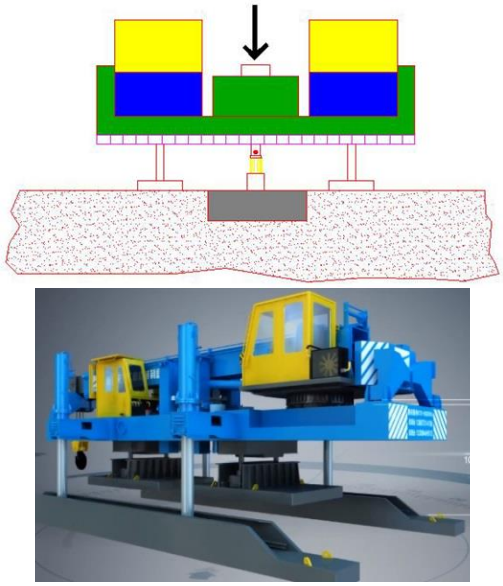

Figure 5 Illustration of full scale static load test on SNSF

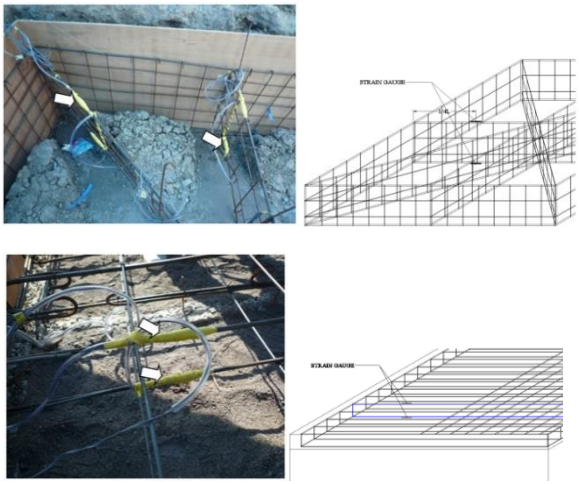

Figure 6 Strain Gauge FLA-5-11 installation at ribs and plate

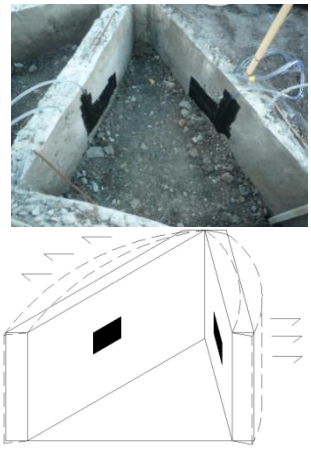

Figure 7 Strain Gauge PL-60-11 installation at construction rib

3.2 Loading Stages Setup

Figure 8 illustrates the loading setting. A kentledge system was utilized that similar to jacked pile installation system. The system was weighted 20% more than the loading applied to avoid its lifting during loading process. The loading was employed by means of hydraulic jack symmetrically to the tested footing. Pressure gauge is installed to record the applied loading during the test. The settlement occurred are recorded by means of 4 displacement gauge. The average value of the recorded settlement is utilized as the settlement data.

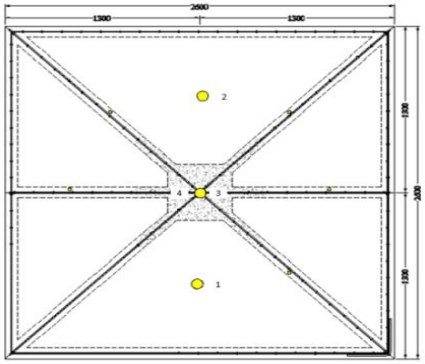

Figure 5 Applied loading location

The SLT complies with ASTM D 1143-81 [8] in which Quick Maintained Load Test and cyclic loading are the applied loading type for the test. The loading process follows the stage shown in Table 4 and Table 5. The points where the loading applied are presented in Figure 5. Point 1 to 3 received 8 Tons loading in order to clarify the elastic condition. The loading was applied at point 1, 3, and 2 sequentially. Meanwhile, the 60 Tons loading was applied to point 4 only to attain failure condition.

Table 4 8 tons loading stage

Cycle 1 Load / Time	Cycle 2 Load / Time
0/-	0/-
2 ton/5 minutes	4 ton/5 minutes
4 ton/5 minutes	8 ton/10 minutes
2 ton/5 minutes	4 ton/5 minutes
0/10 minutes	0/10 minutes

Table 5 60 tons loading stage

Cycle 1 Load / Time	Cycle 2 Load / Time	Cycle 3 Load / Time	Cycle 4 Load / Time
0/-	0/-	0/-	0/-
8 Tons/5 minutes	8 Tons/5 minutes	8 Tons/5 minutes	15 Tons/5 minutes
15 Tons/10 minutes	15 Tons/5 minutes	15 Tons/5 minutes	30 Tons/5 minutes
8 Tons/5 minutes	30 Tons/10 minutes	30 Tons/5 minutes	45 Tons/5 minutes
0/10 minutes	15 Tons/5 minutes	45 Tons/10 minutes	60 Tons/10 minutes
	8 Tons/5 minutes	30 Tons/5 minutes	45 Tons/5 minutes
	0/10 minutes	15 Tons/5 minutes	30 Tons/5 minutes
		8 Tons/5 minutes	15 Tons/5 minutes
		0/10 minutes	0/10 minutes

4.0 TEST RESULTS

The result of 8 ton cyclic loading is shown in Figure **6**. Meanwhile the settlement distribution across the plate can be seen in Figure 10. The applied loading at point 1 induced about 1 mm permanent settlements. Meanwhile, the loading at points 2 and 3 caused 3.2 mm and 6.3 mm permanent settlements respectively. Figure 9 shows clearly that the slope of load-settlement relationships decreased inversely with the applied loading sequence but the permanent settlement was proportional. It can be associated that the increasing of settlement was the accumulation from previous loading so that the permanent settlement of the later loading was always larger than previous stage.

The permanent deformation took account at unloading stage. The induced deformation shows that plastic condition was activated. However, it was less than 5% to the rib width [9]. This condition showed that tip resistant R_{tip} was not fully mobilized and was categorized into small displacement condition. In contrast, when the loading was 4 Tons, the deformation that occurred showed that all those three points were in elastic condition.

The last loading stage was applying cyclic load to failure at point 4. The result is presented in Figure 14. The load cycle was 15, 30, 45, and 60 Tons. The permanent settlements induced when unloading applied were 0.21 mm, 0.88 mm, 2.54 mm, and 20.29 mm. The settlements demonstrate that loading to 45 Tons is still in small displacement zone. The plastic zone was activated when the loading exceeded 45 Tons. When 60 Tons loading applied, the settlements increased to reach asymptotic line that was settlement at the failure loading. It means that the SNSF segment was able to support loading up to 60 Tons or the ultimate bearing capacity was 60 Tons.

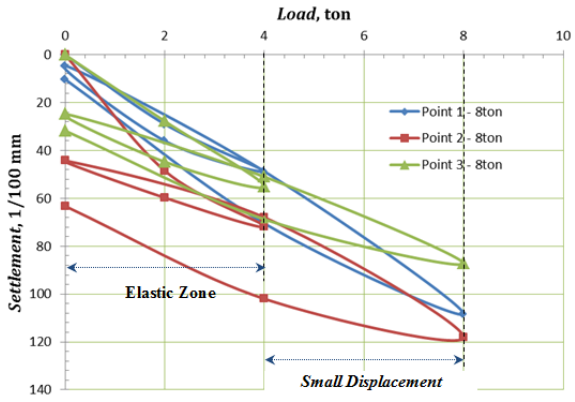

Figure 6 Cyclic loading test (8 Tons)

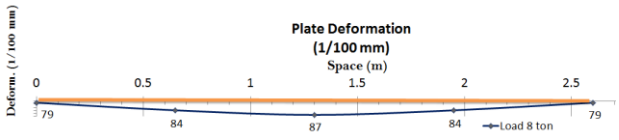

Load 8 Tons

Spasi (m)	Deform. (1/100 mm)
0	79
0.65	84
1.3	87
1.95	84
2.6	79

Figure 7 Plate deformation at point 3 (8 Tons)

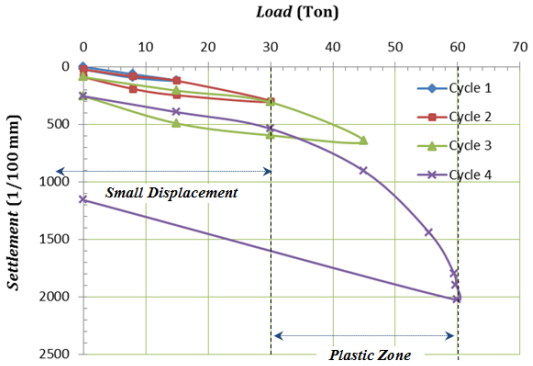

Figure 8 Static loading test till failure - 60 Tons

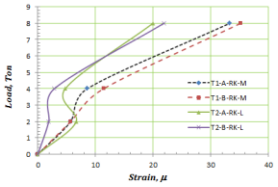

(a). records of strain gauge embeded on diagonal and vertical construction ribs

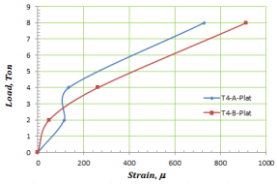

(b). records of strain gauge embedded in the plate

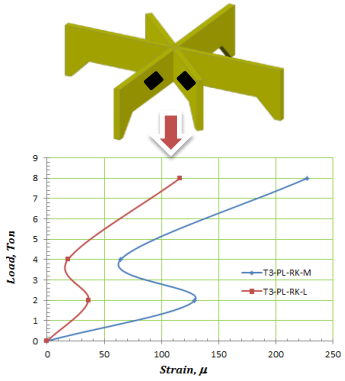

(c). records of strain gauge installed on the concrete surface

Figure 9 Load – strain relationship from strain gauge record at point 3

Strain gauges were installed at both diagonal and vertical construction ribs, the surface of the concrete rib, and at the surface and bottom of the plate. All the strains induced during SLT are under small strain condition (Figure 13 and Figure 14). The strain at construction rib surface was 0.000894 (894 μ) mm/mm. It was even less than 0.003 mm/mm. Since the on spot strain was under small strain condition, then the rib and plate dimension were adjustable. For example: the strain at the plate was 662 μ (Figure 14b). It is identical to tensile stress (10.92 KN). If the distance between compressive-tensile reinforcement was 0.10 m, the working moment becomes 1,092 KN-m. The working moment obtained during SLT will be used for numerical calculation.

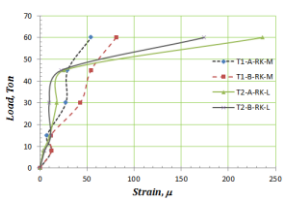

(a). records of strain gauge embeded on diagonal and vertical construction ribs

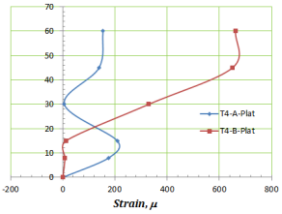

(b). records of strain gauge embedded in the plate

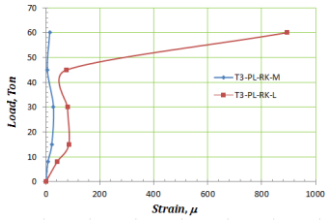

(c). records of strain gauge installed on the concrete surface

Figure 10 Load – strain relationship from strain gauge record at point 4

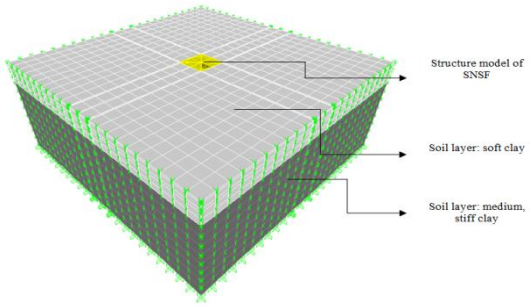

Figure 11 3D SNSF model

5.0 MULATION OF FINITE ELEMENT MODELS

The FEM analysis was conducted to verify the experimental results. Both SAP 3D and PLAXIS 2D were utilized for finite element modeling.

5.1 SAP 3D Simulation Results

3D modeling using structural finite element software SAP 3D was applicable since 30 Tons loading induced small displacement condition (< 5 mm or 5% of rib thickness). However, the model was not applicable for 45 Tons loading that activated plastic condition. The 3D SNSF model is shown in Figure 14. The loading sequence was 8, 15, and 30 Tons at points similar to the full scale SLT.

The displacement induced by the loading on the simulation is shown in Table 6. 8 Tons loading were applied to all points but 15 and 30 Tons were to point 4 only.

5.2 PLAXIS 2D Simulation Results

The SNSF was modeled in PLAXIS 2D as symmetric one. The model is presented in Figure 15. Meanwhile the results can be seen in Figure 16 to Figure 20. The soil parameters input are presented in Table 7.

Concerning the soft soil in the above table, the soil layer had PI value of 35%. It indicates that the soil may be suffering unsaturated condition during seasonal change. Thereby the range of values was used for its shear strength and stiffness to accommodate field condition during sunny season (Table 7).

All the maximum deformations occurred exactly below the SNSF (Figure 16). The deformation pattern agreed with Terzaghi's theory in which active downward displacement below the SNSF followed by horizontal displacement and passive upward displacement next to the footing

The loading-settlement curves can be revealed in Figure 17 and Figure 18. It can be seen clearly that simulation results consistent with SLT ones. However, the simulated permanent deformation occurred for cyclic loading was about 60% of SLT one.

Table 6 Loads versus stresses of SAP model

Point 1					
Loads	Displacement	Stress in Plate (MPa)		Stress in RIB 1 (MPa)	
(Ton)	(1/100 mm)	Tensile	Compressive	Tensile	Compressive
2	35.36	0.0876	-0.2019	0.1462	-0.0532
4	46.35	0.1744	-0.2708	0.2396	-0.0559
8	100.32	0.4482	-0.6324	0.4759	-0.197
Point 2					
Loads	Displacement	Stress in Plate (MPa)		Stress in RIB 1 (MPa)	
(Ton)	(1/100 mm)	Tensile	Compressive	Tensile	Compressive
2	35.48	0.0071	-0.0343	0.1558	-0.0597
4	46.51	0.0126	-0.0456	0.2454	-0.1016
8	100.57	0.0343	-0.0801	0.5419	-0.3000
Point 3					
Loads	Displacement	Stress in Plate (MPa)		Stress in RIB 1 (MPa)	
(Ton)	(1/100 mm)	Tensile	Compressive	Tensile	Compressive
2	37.44	0.0141	-0.0442	0.2552	-0.0514
4	50.04	0.0276	-0.0659	0.3958	-0.1266
8	105.22	0.0652	-0.1811	0.8603	-0.2775
Point 4					
Loads	Displacement	Stress in Plate (MPa)		Stress in RIB 1 (MPa)	
(Ton)	(1/100 mm)	Tensile	Compressive	Tensile	Compressive
8	105.22	0.0652	-0.1811	0.8603	-0.2775
15	119.29	0.1039	-0.1925	1.3390	-0.3272
30	293.74	0.2084	-0.3691	2.4818	-0.6304

Table 7 Soil parameters

Parameters	Name	Soft Clay	Soft Clay -Medium	Unit
Material model	Model	HSM	HSM	-
Type of material behavior	Type	Undrained	Undrained	-
Dry soil weight	γ_{dry}	11	12.50	KN/m^3
Wet soil weight	γ_{wet}	17	17.50	KN/m^3
Permeability in horizontal direction	k_x	0.0001	0.0001	m/day
Permeability in vertical direction	k_y	0.0001	0.0001	m/day
Cohesion (constant)	c_{ref}	26.0 – 35.0	27	KN/m^2
Friction angle	φ	35	14	°
Dilatancy angle	ψ	0.0	0.0	°
Young's modulus (ref-50)	E_{50}^{ref}	7500 - 10500	25000	KN/m^2
Young's modulus (ref-oed)	E_{oed}^{ref}	7500 - 10500	25000	KN/m^2
Young's modulus (ref-ur)	E_{ur}^{ref}	22500	75000	KN/m^2
Power	m	0.5	0.5	

Parameters	Name	Soft Clay	Soft Clay -Medium	Unit
Poisson Ratio (ur)	υ_{ur}	0.2	0.3	
Reference Stress	p_{ref}	100	100	KN/m^2
Strength reduction factor inter.	R_{inter}	0.7	0.7	-

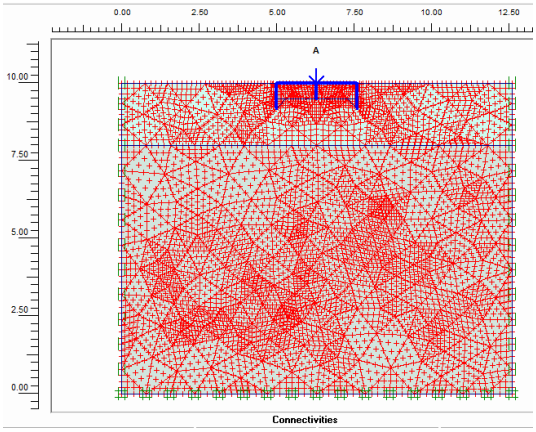

Figure 12 2D symmetrical model on PLAXIS 2D

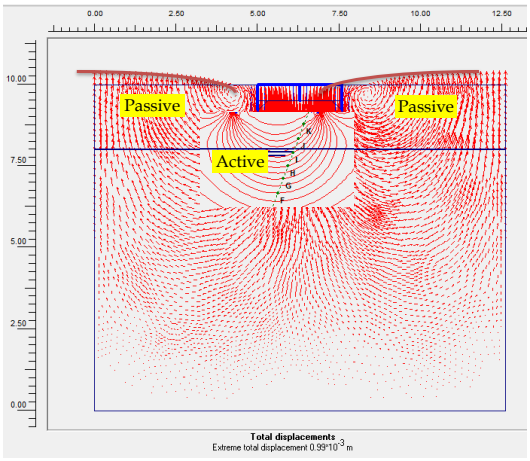

Figure 13 Displacement distribution for 8 tons loading

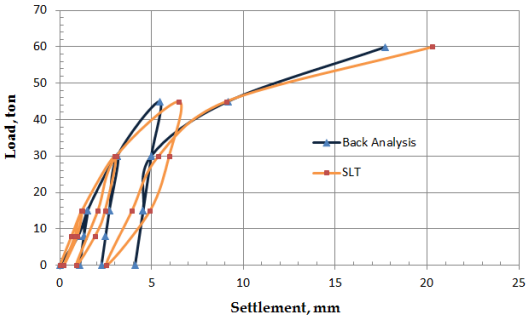

Figure 14 Load – settlement curves for cyclic loading condition

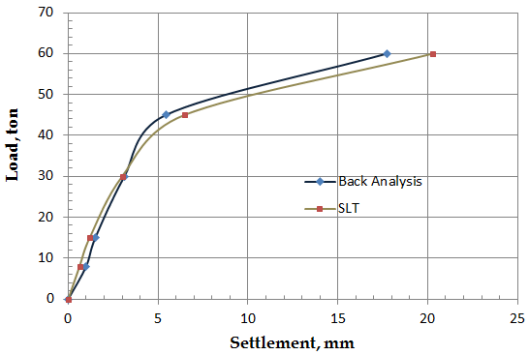

Figure 15 Comparison of SLT and numerical model result

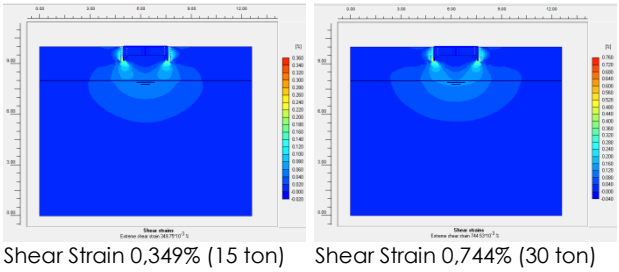

Shear Strain 0,349% (15 ton) Shear Strain 0,744% (30 ton)

Figure 16 Shear strain distribution for 15 and 30 Tons loading

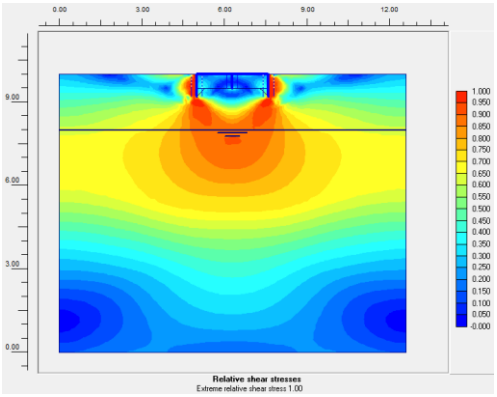

Figure 17 Relative Shear Stresses distribution for 60 Tons loading

Figure 19 shows shear strain distribution for various loading condition. The figures show that the bearing capacity at the tip of construction rib was in plastic condition. It is supported by the relative shear stress condition which is the ratio between shear stress to its associated failure envelope value (Figure 20).

The detail comparison between the simulation results and SLT can be seen in Table 8 Significant

differences occurred when the loading was 30 Tons. It may be associated with the permanent deformation during cyclic loading at SLT that led into accumulated deformation at the end of loading, though it was at small displacement condition. Meanwhile, SAP 3D consider elastic condition for structural material. Therefore the modification of the structural dimension was adjustable during cyclic loading simulation.

Table 8 The comparison between SLT and numerical model results

Load (ton)	SAP 3D (mm)	PLAXIS 2D (mm)	SLT (mm)	Note
8	0.75	0.99	0.63	Small displacement
15	1.19	1.5	1.20	
30	2.14	3.13	3.00	

6.0 DISCUSSION

6.1 Load Transfer Mechanism

Load transfer mechanism is very important to explore stress distribution during loading on SNSF and the soil stratum below it. Based on the SLT results, the load at SNSF first carried by the plate then transferred it to the ribs and received by the soil stratum through the tip of the rib. When the working load increased, the load was also distributed by the plate to the filled soil that transferred to the existing soil below. The SLT result succeeded to explore the load transfer mechanism occurred at SNSF.

Full scale SLT result confirmed that the strain induced at rib reinforcement, plate, and the surface of the rib were very small and involved into small strain condition.

6.2 Back Analysis of Bearing Capacity

Back analysis was conducted to verify the SLT results by means numerical modeling. SNSF comprises of construction ribs, settlement ribs, and floor plate. The dimension of the SNSF is presented in Table 9.

The value of cu was 2/3 NSPT (20 kPa). The N_c was obtained Terzaghi and Peck [10] and pile bearing capacity factor α was determined using American Petroleum Institute (API) [11] procedure. The soil bearing capacity was calculated based on the load transfer mechanism occurred. The first bearing capacity computed was the tip resistant followed by plate and filled soil to the soil stratum. The results are shown in Table 10.

Table 9 SNSF dimensions and soil parameters

A_{RK} (m^2)	A_{RS} (m^2)	A_{Tip} (m^2)	A_{Plate} (m^2)	N_c	N_γ	c_u (kPa)	α	Note
7.63	7.36	1.57	4.19	5.14	0.0	20	1	Subgrade
7.63	7.36	1.57	4.19	5.14	0.0	40	0.8	Fill soil
7.63	7.36	1.57	4.19	5.14	0.0	60	0.6	

Table 10 Soil baring capacity of SNSF

Q_{Rib}			Q_{Pelat} (Ton)	$Q_{Rib + Pelat}$ (Ton)	N_{SPT}
$Q_{Rib-Tip}$ (Ton)	$Q_{Rib-Sisi}$ (Ton)	$Q_{Rib-Total}$ (Ton)			
16.19	29.98	46.17	55.94	102.10	3
16.19	47.97	64.16	111.87	176.03	6
16.19	53.97	70.15	167.81	237.96	9

Table 11 L-URF for various loading (N_{SPT} = 3)

Load (Ton)	Load-Ultimate Ratio Factor (LURF)				
	Rib			Plate	Rib + Plate
	R_{Tip}	R_{Shaft}	R_{Total}		
8	2.02 (16.19/8)	3.75 (29.98/8)	5.77 (46.17/8)	6.99 (55.94/8)	12.76 (102.10/8)
15	1.08	2,00 (29.98/15)	3.08	3.73	6.81
30	0.54	1.00	1.54	1.86	3.40 (102.10/30)

According to Table 10, the information about the stress induced on the SNSF elements during loading is necessary. Safety factor to the ultimate bearing capacity can be utilized to show that information.

The authors proposed Load-Ultimate Ratio Factor (L-URF) which is the ratio between ultimate bearing capacity and ultimate load to represent the stress induced at SNSF elements. SLT results show that soil failed when the loading was 60 Tons. It means that ultimate load carried by the soil is 60 Tons. The L-URF value is 102.6/60 = 1.71. This value becomes a reference to set the load transfer mechanism for filled soil with density similar to NSPT = 3. L-URF for SNSF elements can be reveal in Table 11.

It can be seen clearly that when the loading was 8 Tons, R_{Tip} was 2.02 which is more than 1.71. It means that all the loading is carried by the tip of the rib. When the loading increases to 15 Tons, R_{Tip} reduced to 1.08 while the shaft resistant R_{Shaft} was still more than the reference value. It confirmed that the rib friction resistant started to be initiated. Finally, all the elements were activated to bear the 30 Tons loading.

Furthermore, the effects of the height of both construction and settlement ribs on SNSF were analyzed theoretically. The effects of the ribs thickness was also considered as well. The calculation result of SNSF bearing capacity for various ribs height and thickness are presented in Table 12 and Table 13. It can be seen clearly that variation of the ribs height has slightly effects on the SNSF bearing capacity. In contrast, the ribs thickness modifies it significantly.

Table 12 $Q_{Ultimate}$ for various heights of the ribs

Height of Rib (m)	Rib		
	R_{Tip} (Ton)	R_{Shaft} (Ton)	R_{Total} (Ton)
0.5	16.19	29.98	46.17
0.6	16.19	33.03	49.22
0.7	16.19	36.09	52.27

Table 13 $Q_{Ultimate}$ for various ribs thickness

Width of rib (m)	Rib		
	R_{Tip} (Ton)	R_{Shaft} (Ton)	R_{Total} (Ton)
0.1	16.19	29.98	46.17
0.2	31.14	28.94	60.08
0.3	44.86	27.90	72.76

6.0 CONCLUSION

A full scale static load test and numerical analysis on Spider net System Footing was described. The results led to the conclusion as follows:

1. Load transfer mechanism on SNSF was explored. When the loading is relatively small, it is fully carried by the tip of the rip and transferred to the soil stratum below. Increasing the loading, the shift resistance of the rib is initiated and supported the tip of the rib carrying the working load. Finally, the plate and filled soil is activated and transmit the loading to the soil stratum below the system. When this condition is achieved, all elements of SNSF is working as a system sustaining the applied load.
2. The depth of the rib has no significant effect to the bearing capacity of SNSF.
3. The thickness of the rib increases the SNSF performance significantly as well as the density of the filled soil.
4. The numerical analysis by means of SAP 3D and PLAXIS 2D succeed to model the SNSF and the simulation results was consistent with SLT ones.

Acknowledgement

The first author acknowledges the scholarships provided by DIKTI to support this research and his doctorate study

References

[1] Suhendro, B. 1992. Progress report III: Optimation Study on The Equation of Chicken Claws System Footing. Civil Engineering Department, Gadjah Mada University, Yogyakarta (in Indonesian).
[2] Hardiyatmo, H. C., Suhendro, B. dan Adi, A. D. 2000. The Behavior Of Chicken Claws Footing: The Constribution On Design. Research Report. Lembaga Penelitian Universitas Gajah Mada, Yogyakarta.
[3] Anderson, J., Townsend, F. and Rahelison, L. 2007. Load Testing and Settlement Prediction of Shallow Foundation. *J. Geotech. Geoenviron. Eng*. 133(12): 1494–1502.
[4] Srilakshmi G. and Rekha, B. 2011. Analysis of MAT Foundation using Finite Element Method. *International Journal of Earth Sciences and Engineering*. 4(6):113-115.
[5] Djajaputra, A., Sofwan, A., Rahardian, H., Pane, I., Taufik, R. and Rukmono, A. 2009. Application of Spider Net System Footing on Runaway, Taxiway, and Container Yard of Airport. Research Report, Penelitian Hibah - Program Insentif Peningkatan Kapasitas IPTEK Sistem Produksi.
[6] Anonim. (2008a). Technical Resume: The Spider Net System Footing (SNSF), The Expansion Of Juwata Airport, Tarakan, East Kalimantan. Katama, Co Ltd. Jakarta (in Indonesian).
[7] Sridharan, A. and Prakash, K. 2000. Classification Procedures For Expansive Soils. *Proceedings of the ICE - Geotechnical Engineering*. 143(4): 235 –240.
[8] ASTM. 1994. Standard Test Method For Piles Under Static Axial Compressive Load. D1143, West Conshohocken, PA.
[9] Institution of Civil Engineers. 2012. ICE Manual of Geotechnical Engineering. II. ICE Publishing. London, UK.
[10] Terzaghi, K. dan Peck, R. B. 1967. Soil Mechanics in Engineering Practice. Wiley, New York, USA.
[11] American Petroleum Institute (API). 1994. Standard Method of Testing Piles under Axial Compressive Load. Annual Book of API Standards.